JOURNAL OF AGRICULTURAL AND FOOD CHEMISTRY

Structural Elucidation of T-2 Toxin Thermal Degradation Products and Investigations toward Their Occurrence in Retail Food

MARITA BEYER,[†] INES FERSE,[†] DENNIS MULAC,[†] ERNST-ULRICH WÜRTHWEIN,[‡] AND HANS-ULRICH HUMPF*,[†]

Institut für Lebensmittelchemie, Westfälische Wilhelms-Universität Münster, Corrensstrasse 45, D-48149 Münster, Germany, and Organisch-Chemisches Institut, Westfälische Wilhelms-Universität Münster, Corrensstrasse 40, D-48149 Münster, Germany

The stability of T-2 toxin under the conditions of baking or cooking was investigated using heating experiments with the model substances α-D-glucose, α-D-methyl-glucopyranosid, *N*-α-acetyl-L-lysine methyl ester, and *N*-α-acetyl-cysteine methyl ester. The reaction residue was screened for degradation products using gas chromatography−mass spectrometry (GC−MS) and high-performance liquid chromatography with evaporative light-scattering detection (HPLC−ELSD). Although T-2 toxin was degraded under all conditions, only heating of T-2 toxin with α-D-glucose produced a mixture of three degradation products, which were isolated and identified by MS and nuclear magnetic resonance (NMR) experiments. The reaction mechanism for the formation of the T-2 degradation products was elucidated by quantum chemical calculations. The relevance of these degradation products was investigated by baking experiments as well as the analysis of retail food samples. In cell-culture studies using immortalized human kidney epithelial (IHKE) cells, the T-2 degradation products were less cytotoxic (formazan dye cytotoxicity assay) compared to T-2 toxin.

KEYWORDS: T-2 toxin; mycotoxin; trichothecene; thermal degradation; food processing; degradation products; heating; stability; GC−MS; HPLC−MS/MS; thermal-treated food; food safety; toxicity

INTRODUCTION

Molds of the *Fusarium* genus are crop pathogens, which predominantly infect living plants during their period of growth. Thus, an infection with *Fusaria* is always accompanied by losses during harvest and reduction in quality. In addition, infected plants are contaminated with mycotoxins, toxic secondary metabolites. Mycotoxins produced by fungi of the *Fusarium* genus are fumonisins and zearalenone, as well as the large group of trichothecenes, whose most prominent representatives are deoxynivalenol, T-2 toxin (T-2), and HT-2 toxin (HT-2). T-2 and HT-2 are type-A trichothecenes, while deoxynivalenol belongs to the group of type-B trichothecenes. Both subgroups vary at C-8, where type-B trichothecenes are characterized by a keto group and type-A trichothecenes are esterified, hydroxylated, or non-substituted (**Figure 1**) (*1*). In Europe, especially in the nordic countries, the contamination of cereals with T-2 and HT-2 is a serious problem. Although the concentrations of deoxynivalenol (and nivalenol) are often higher than those of T-2 and HT-2, these toxins pose a risk for human health because of the higher toxicity of type-A trichothecenes. The general toxicity of trichothecenes is attributed to the noncompetitive inhibition of the protein biosynthesis in eukaryotic cells by affecting the ribosomal function (*2*). T-2 and HT-2, which differ only at C-4, show a higher acute toxicity in comparison to deoxynivalenol. The LD_{50} (i.p., mice) value of T-2 is 9.1 mg/kg bw, and its major *in vivo* metabolite HT-2 has a LD_{50} value of 10.0 mg/kg bw (*3*), which is in the same dose range. Because the toxicity of T-2 *in vivo* is at least partly attributed to the major metabolite HT-2, a combined TDI of 0.06 μg/kg bw was set for the sum of T-2 and HT-2 (*4*). In food samples, T-2 is frequently found in combination with HT-2, whereby various cereal crops (*4*) but especially oats and oat products (*5*) are contaminated. In the 1940s, many people in the former USSR showed symptoms of alimentary toxic aleukia (ATA) after eating overwintered grain colonized with *F. sporotrichioides* and *F. poae*, which are the main producers of T-2 (*6*). The

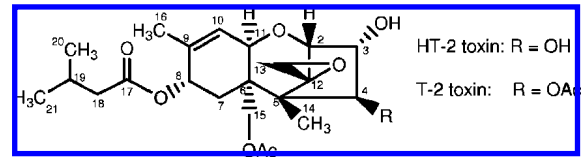

Figure 1. Structures of type-A trichothecenes T-2 toxin **1** and HT-2 toxin **2**.

* To whom correspondence should be addressed. Telephone: +49-251-83-333-91. Fax: +49-251-83-333-96. E-mail: humpf@uni-muenster.de.

[†] Institut für Lebensmittelchemie.

[‡] Organisch-Chemisches Institut.

10.1021/jf803516s CCC: $40.75
Published on Web 02/05/2009

weight of evidence indicates that T-2 was likely a causative agent of this human disease.

Because T-2 is a molecule with high toxicity often found in food samples, it is important to investigate the stability of this compound under food-processing conditions with a special focus on the formation of degradation products and their cytotoxicity. In general, trichothecenes are relatively stable compounds (*4*); nevertheless, their complete degradation has been observed by heating for 30−40 min at 210 °C (*7*). Thus far, most of the studies toward the stability of trichothecenes under typical food-processing conditions, such as cooking or baking, deal with deoxynivalenol, partially including nivalenol. In different studies, it has been shown that both molecules are degraded under food-processing conditions (*8, 9*), whereby the degree of degradation is dependent upon the temperature, time, and additives (*10*). For instance, deoxynivalenol and nivalenol are degraded under alkaline conditions (*11, 12*), which prevail in the preparation of tortillas (*13*). In this process, several degradation products are generated, whereby the most important degradation products of deoxynivalenol are nordeoxynivalenol A, nordeoxynivalenol B, and nordeoxynivalenol C. These degradation products were detected in different cereal samples, and they are less cytotoxic compared to deoxynivalenol in cell-culture assays (*11*). However, on the basis of structural differences, comparable degradation products cannot be generated with T-2. Because of ester hydrolysis, the amount of T-2 decreases as well under alkaline conditions and HT-2, T-2 triol, and T-2 tetraol are formed. Cell-culture studies by our group with two different types of human cells in primary culture recently showed that HT-2 is nearly as toxic as T-2, while T-2 triol as well as T-2 tetraol are less cytotoxic (*14*). T-2 triol plays only a minor role in food samples, but the concentration levels of T-2 tetraol are often equal or even higher than those of T-2 (*15*).

To investigate the influence of food matrices on the stability of T-2 under typical food-processing conditions, we performed heating experiments with model substances. By doing so, we simulated important and reactive food constituents to identify degradation and reaction products as well as the binding of T-2 to food constituents. This model system was already used to study the degradation of fumonisins (*16*) as well as deoxynivalenol and nivalenol (*11, 12*). T-2 was heated with α-D-glucose as a sugar model, methyl-α-D-glucopyranoside as a starch model, and the amino acid derivates *N*-α-acetyl-L-lysine methyl ester and *N*-α-acetyl-cysteine methyl ester as protein models. The reaction residues were screened for degradation products by gas chromatography−mass spectrometry (GC−MS) and high-performance liquid chromatography coupled to an evaporative light-scattering detector (HPLC−ELSD).

MATERIALS AND METHODS

Reagents. All solvents and reagents were purchased from VWR (Darmstadt, Germany) or Sigma-Aldrich (Deisenhofen, Germany). T-2 was produced by inoculating maize media with *F. sporotrichioides* (DSM 62423) and grown for 21 days at 15 °C, followed by extraction with methanol/water (70:30, v/v). Further purification was achieved using centrifugal partition chromatography with a solvent system of water/methanol/acetonitrile/*tert*-butyl methyl ether/ethyl acetate/pentane (2:1:1:1:1:2) followed by crystallization. Water for HPLC separation was purified with a MilliQ Gradient A10 system (Millipore, Schwalbach, Germany).

Model Experiments. The following compounds were used as food models: α-D-glucose as a sugar model, methyl-α-D-glucopyranoside as a starch model, and the amino acid derivates *N*-α-acetyl-L-lysine methyl ester and *N*-acetyl-L-cysteine methyl ester as protein models (*16*). The experiments were performed by heating 100 μg of T-2 with 1 mg of model compound without solvent. To obtain a homogeneous mixture, aliquots of the stock solutions of the reactants (1−10 mg/mL in acetonitrile) were vortexed in a 1.5 mL glass vial and the solvent was removed under a stream of nitrogen. The mixture was heated in a heating block for various periods (20−60 min) at different temperatures (150−200 °C). The residue was further analyzed by GC−MS and HPLC−ELSD. As a control, pure T-2 toxin was heated under the conditions described above.

HPLC−ELSD. The reaction residue was resolved in acetonitrile/water (50:50, v/v) and separated on a 250 × 4.6 mm i.d., 5 μm, Synergi Fusion column (Phenomenex, Aschaffenburg, Germany) using a binary gradient delivered by a Shimadzu LC-10AT pump with water and acetonitrile as eluents. The HPLC was programmed as follows: isocratic step at 10% solvent acetonitrile for 1 min; at 10 min, the content of acetonitrile was 50%; and at 20 min, it was 100% acetonitrile, which was held for 10 min. After each HPLC run, the column was equilibrated for 10 min at the starting conditions. The flow rate was 1 mL/min. The compounds were detected with a Polymer Laboratories PL-ELS 2100 evaporative light-scattering detector (Varian, Darmstadt, Germany). The ELSD parameters were set as follows: gas flow rate, 1.6 L/min; nebulizer temperature, 40 °C; evaporator temperature, 60 °C.

GC−MS. Gas chromatography electron impact mass spectrometry (GC−EI−MS) data were acquired on a HP6890 series gas chromatograph coupled to a HP5973 mass spectrometer (Hewlett-Packard, Böblingen, Germany) after derivatization of the compounds with 200 μL of trimethylsilylimidazole (TMSI, 70 °C, 30 min) and the addition of 400 μL of *tert*-butyl methyl ether. Data acquisition was performed with the Chemstation software (Agilent). Chromatographic separation was performed on a 60 m × 0.25 mm i.d. fused silica, 0.25 μm, Chrompack 5861 CP-SIL 8 CB column (Chrompack, Middelburg, The Netherlands) using 1 mL/min helium as a carrier gas. The injector temperature was set at 250 °C, and the injection volume was 1 μL with split injection (1:9). The column temperature was held initially at 100 °C for 1 min and then programmed at 4 °C/min to 260 °C, which was then held constant for 10 min. The transfer line was heated at 320 °C. The mass spectrometer was operated in the electron impact mode (EI, 70 eV electron energy) with a source temperature of 230 °C, and the quadrupole was heated at 150 °C. Mass spectra were acquired in the full-scan mode ranging from *m*/*z* 40−800 with a scan rate of 2.0 scans/s.

Preparation and Isolation of T-2 Degradation Products. A total of 10 mg of crystalline T-2 and 100 mg of α-D-glucose were weighed in a 4 mL glass vial and dissolved in 1 mL of acetonitrile/water (1:1, v/v). After vigorous mixing, the solvent was removed under a stream of nitrogen at 60 °C. The glass vial was closed and heated for 6 h under atmospheric conditions at 200 °C in a heating block. The cooled reaction residue was resolved in acetonitrile/water (1:1, v/v) and separated on a 300 × 19 mm i.d., 7 μm, Symmetry Prep C_8 column (Waters, Eschborn, Germany) using a binary gradient delivered by a Varian Pro Star M-210 pump with water and acetonitrile as eluents. The HPLC was programmed as follows: isocratic step at 10% solvent acetonitrile for 1 min; 10 min, 50% acetonitrile; and 20 min, 100% acetonitrile. The flow rate was 15 mL/min, and the HPLC eluate was fractionized (12−22 min; fraction time, 15 s; 40 fractions). Fractions were checked via HPLC−MS, and selected fractions were combined.

HPLC−ESI−MS Analysis. For HPLC−ESI−MS analysis, an Agilent 1200 series HPLC was linked to an API 3200 mass spectrometer. Data acquisition was performed with the Analyst 1.4.2 software (Applied Biosystems, Darmstadt, Germany). Chromatographic separation was performed on a 150 × 2.1 mm i.d., 4 μm, Phenomenex Synergi Fusion column (Phenomenex, Aschaffenburg, Germany) using a linear binary gradient with water and acetonitrile as eluents. The injection volume was 5 μL, and the flow rate was 200 μL/min. The HPLC was programmed as follows: isocratic step at 10% acetonitrile for 1 min, followed by a linear gradient to 100% acetonitrile in 26 min. After each HPLC run, the column was washed with 100% acetonitrile for 7 min and equilibrated for 15 min at the starting conditions. For HPLC−MS, the mass spectrometer was operated in the Q1 MS mode

detecting positive ions (200−800 amu), whereby the ion spray voltage was set at 5500 V. Zero-grade air served as the nebulizer gas (30 psi) and heated at 300 °C, as turbo gas for solvent drying (50 psi).

Exact Mass Measurements. The exact masses of the degradation products were measured on a Bruker Micro-TOF (Bruker Daltronics, Bremen, Germany) mass spectrometer with flow injection and referenced on sodium formiate. The compounds were dissolved in 1 mL of MeOH, and 10 μL of a saturated solution of $NaBF_4$ in MeOH was added to measure the exact mass of the sodium adducts. The resolution of the mass spectrometer was R_{fwhm} 10 000 (full width at half-maximum).

Electrospray Ionization (ESI)−MS/MS. ESI mass and product ion spectra were acquired on an API 4000 QTrap mass spectrometer (Applied Biosystems, Darmstadt, Germany) with direct flow infusion. For electrospray ionization, the ion voltage was set at −4500 V in the negative mode and 5500 V in the positive mode. Nitrogen served as curtain gas (20 psi); the declustering potential, being the accelerating voltage from atmospheric pressure into high vacuum, was set at −50 V in the negative mode and 50 V in the positive mode. The MS/MS parameters were dependent upon the substances, detecting the fragmentation of the $[M + NH_4]^+$ molecular ions into specific product ions after the collision with nitrogen (4.5×10^{-5} Torr). The collision energies are given at the respective compounds.

NMR Spectroscopy. NMR data were acquired on a Bruker DPX-400 (Bruker BioSpin, Rheinstetten, Germany) or a Unity plus (Varian, Palo Alto, CA) NMR spectrometer. Signals are reported in parts per million relative to d_4-MeOD (compounds **1** and **2**) or $CDCl_3$ (compound **3**). For structural elucidation and NMR signal assignment, 2D NMR experiments, such as gradient-selected correlated spectroscopy, heteronuclear multiple-quantum correlation (HMQC), heteronuclear multiple-bond correlation (HMBC), and distortionless enhancement by polarization transfer experiments using a 135° decoupler pulse (DEPT-135), as well as 1D nuclear Overhauser enhancement (NOE) spectroscopy were performed. Pulse programs for the experiments were taken from the software library.

Spectroscopy Data. Compound **1**: 4,15-diacetoxy-10,12-cyclohexa-(10*H*)-3,9,12-trihydroxy-8-[3-methylbutyryloxy]-trichothecene. Found: *m*/*z* 507.2217. Calculated for $C_{24}H_{36}O_{10} + Na^+$: 507.2206.

EI−MS (silylated compound **1**, diastereomer 1) (70 V) *m*/*z* (%): 73 (100), 57 (54), 43 (43), 85 (42), 75 (30), 117 (28), 143 (24), 271 (17), 640 (10) [M^+].

EI−MS (silylated compound **1**, diastereomer 2) (70 V) *m*/*z* (%): 73 (100), 43 (47), 75 (46), 57 (34), 117 (32), 85 (26), 159 (21), 143 (19), 256 (17), 271 (13), 640 (11) [M^+].

ESI−MS (mixture of both diastereomers) positive mode *m*/*z* 502.5 $[M + NH_4]^+$, MS/MS (25 V): 383 (100), 425 (93), 407 (58), 263 (51), 365 (31), 502 (28), 305 (24), 245 (20), 323 (20), 347 (20).

^{1}H NMR (600 MHz, d_4-MeOD) δ: 0.96 (6H, d, J = 6.7, H-20/21), 1.10 (3H, s, H-14), 1.17 (3H, s, H-16), 1.57 (1H, dd, $J_{7A,8}$ = 11.4, $J_{A,B}$ = 14.0, H-7A), 1.59 (1H, dd, $J_{13A,10}$ = 5.5, $J_{A,B}$ = 14.3, H-13A), 1.88 (1H, dd, $J_{13B,10}$ = 12.3, $J_{A,B}$ = 14.3, H-13B), 2.06 (3H, s, Ac-CH_3), 2.06 (3H, s, Ac-CH_3), 2.11 (1H, m, H-19), 2.16 (1H, dd, $J_{7B,8}$ = 5.3, $J_{A,B}$ = 14.0, H-7B), 2.27 (2H, m, H-18), 2.30 (1H, m, $J_{10,11}$ = 4.0, $J_{10,13A}$ = 5.5, $J_{10,13B}$ = 12.3, H-10), 3.74 (1H, d, $J_{11,10}$ = 4.0, H-11), 3.75 (1H, d, $J_{2,3}$ = 4.3, H-2), 3.81 (1H, d, $J_{A,B}$ = 11.4, H-15A), 4.22 (1H, dd, $J_{3,4}$ = 2.2, $J_{3,2}$ = 4.3, H-3), 4.64 (1H, d, $J_{A,B}$ = 11.5, H-15B), 5.06 (1H, dd, $J_{8,7B}$ = 5.3, $J_{8,7A}$ = 11.8, H-8), 5.19 (1H, d, $J_{4,3}$ = 2.2, H-4).

^{13}C NMR (100 MHz, d_4-MeOD) δ: 9.5 (C-14), 19.5 (CH_3 [Ac]), 19.5 (CH_3 [Ac]), 21.3 (C-20), 21.3 (C-21), 22.1 (C-16), 25.4 (C-19), 27.7 (C-13), 31.9 (C-7), 42.7 (C-10), 44.3 (C-18), 45.9 (C-6), 51.6 (C-5), 68.3 (C-11), 71.4 (C-15), 71.7 (C-8), 72.5 (C-9), 76.7 (C-12), 78.2 (C-3), 80.2 (C-2), 84.7 (C-4), 170.8 (C═O [Ac]), 171.8 (C═O [Ac]), 173.3 (C═O [ester]).

NMR data for diastereomer 2 are not shown.

Compound **2**: 4,15-diacetoxy-10,12-cyclohexa-(10*H*)-3,12-dihydroxy-8-[3-methyl-butyryl-oxy]-9-methylidenetrichothecene. Found: *m*/*z* 489.2127. Calculated for $C_{24}H_{34}O_9 + Na^+$: 489.2101.

EI−MS (silylated compound **2**) (70 V) *m*/*z* (%): 73 (100), 43 (61), 57 (38), 75 (30), 117 (29), 85 (22), 143 (19), 41 (13), 257 (11), 245 (10), 74 (9), 129 (9), 550 (9) [M^+].

ESI−MS positive mode *m*/*z* 484.5 $[M + NH_4]^+$, MS/MS (25 V): 305 (100), 246 (38), 226.9 (27), 263 (27), 365 (25), 306 (23), 227.2 (21), 287.3 (19), 286.9 (13), 200 (8).

^{1}H NMR (400 MHz, d_4-MeOD) δ: 0.97 (6H, d, J = 6.7, H-20/21), 1.14 (3H, s, H-14), 1.23 (1H, dd, $J_{7A,8}$ = 11.8, $J_{A,B}$ = 13.9, H-7A), 1.26 (1H, dd, $J_{13A,10}$ = 8.9, $J_{A,B}$ = 14.4, H-13A), 1.80 (1H, dd, $J_{13B,10}$ = 4.9, $J_{A,B}$ = 14.4, H-13B), 2.05 (Ac-CH_3), 2.07 (Ac-CH_3), 2.10 (1H, m, H-19), 2.28 (2H, m, H-18), 2.46 (1H, dd, $J_{7B,8}$ = 5.9, $J_{A,B}$ = 13.9, H-7B), 3.09 (1H, m, $J_{10,11}$ = 4.4, $J_{10,13B}$ = 4.9, $J_{10,13A}$ = 8.9, H-10), 3.27 (1H, d, $J_{2,3}$ = 4.0, H-2), 3.80 (1H, d, $J_{11,10}$ = 4.4, H-11), 3.81 (1H, d, $J_{A,B}$ = 11.5, H-15A), 4.22 (1H, dd, $J_{3,4}$ = 2.2, $J_{3,2}$ = 4.0, H-3), 4.64 (1H, d, $J_{A,B}$ = 11.5, H-15B), 4.90 (2H, d, $J_{A,B}$ = 15.9, H-16), 5.22 (1H, d, $J_{4,3}$ = 2.2, H-4), 5.71 (1H, dd, $J_{8,7B}$ = 5.8, $J_{8,7A}$ = 11.8, H-8).

^{13}C NMR (100 MHz, d_4-MeOD) δ: 9.2 (C-14), 19.4 (CH_3 [Ac]), 19.5 (CH_3 [Ac]), 21.3 (C-20), 21.3 (C-21), 25.5 (C-19), 29.4 (C-13), 36.7 (C-7), 42.6 (C-18), 42.8 (C-10), 46.3 (C-6), 51.7 (C-5), 68.3 (C-8), 71.0 (C-15), 72.5 (C-11), 75.9 (C-13), 78.1 (C-3), 80.2 (C-2), 84.6 (C-4), 106.1 (C-16), 146.0 (C-9), 170.8 (C═O [Ac]), 171.5 (C═O [Ac]), 172.3 (C═O [ester]).

Compound **3**: 4-acetoxy-9,10-cyclopropyl-3,15-dihydroxy-8-[3-methylbutyryl-oxy]-12-oxotrichothecene. Found: *m*/*z* 489.2104. Calculated for $C_{24}H_{34}O_9 + Na^+$: 489.2101.

EI−MS (silylated compound **3**) (70 V) *m*/*z* (%): 118 (100), 43 (52), 57 (46), 73 (35), 85 (31), 136 (20), 107 (18), 119 (17), 117 (15), 75 (15), 41 (14), 280 (11).

ESI−MS positive mode *m*/*z* 484.5 $[M + NH_4]^+$, MS/MS (20 V): 245 (100), 305 (94), 366 (94), 145 (83), 190 (83), 227 (83), 189 (78), 306 (67).

^{1}H NMR (400 MHz, $CDCl_3$) δ: 0.59 (dd, 1H, $J_{A,B}$ = 5.4, $J_{13A,10}$ = 9.4, H-13A), 0.84 (t, 1H, $J_{13B,10}$ = 5.4, $J_{A,B}$ = 5.4, H-13B), 0.96 (s, 3H, H-14), 0.97 (d, 6H, J = 6.3, H-20/21), 1.05 (s, 3H, H-16), 1.25 (m, 1H, $J_{10,13B}$ = 5.4, $J_{10,11}$ = 8.1, $J_{10,13A}$ = 9.4, H-10), 1.42 (dd, 1H, $J_{7A,8}$ = 4.8, $J_{A,B}$ = 15.4, H-7A), 1.51 (m, 1H, $J_{7B,11}$ = 1.6, $J_{7B,8}$ = 4.8, $J_{A,B}$ = 15.4, H-7B), 2.10 (s, 3H, Ac-CH_3), 2.12 (s, 3H, Ac-CH_3), 2.18 (m, 2H, H-18), 3.91 (dd, 1H, $J_{3,4}$ = 2.8, $J_{3,2}$ = 5.0, H-3), 3.93 (d, 1H, $J_{2,3}$ = 5.0, H-2), 4.08 (d, 1H, $J_{A,B}$ = 12.8, H-15A), 4.42 (d, 1H, $J_{A,B}$ = 12.8, H-15B), 4.76 (dd, 1H, $J_{11,7B}$ = 1.6, $J_{11,10}$ = 8.1, H-11), 5.16 (t, 1H, $J_{8,7A}$ = 4.8, $J_{8,7B}$ = 4.8, H-8), 5.75 (d, 1H, $J_{4,3}$ = 2.8, H-4).

^{13}C NMR (100 MHz, $CDCl_3$) δ: 8.1 (C-14), 14.1 (C-13), 17.4 (C-9), 20.7 (C-16), 20.8 (CH_3 [Ac]), 21.1 (CH_3 [Ac]), 22.4 (C-20), 22.4 (C-21), 25.6 (C-19), 26.3 (C-7), 29.7 (C-10), 43.6 (C-18), 50.9 (C-6), 57.2 (C-5), 66.5 (C-11), 69.2 (C-8), 74.4 (C-3), 77.9 (C-2), 81.4 (C-4), 170.2 (C═O [Ac]), 171.7 (C═O [Ac]), 172.1 (C═O [ester]), 209.6 (C-12).

Quantum Chemical Calculations. First, the minima for the reactant and the product were localized using the PM6 method (*17*) as implemented in the MOPAC 2007 (*18*) program. From the minima transition states, structures were obtained by reaction pathway calculations. Using these semi-empirical structures, DFT computations were performed using the Gaussian 03 suite of programs (*19*). The Becke three-parameter exchange functional and the correlation functional of Lee, Yang, and Parr (B3LYP) with the 6-31G(d) basis set were used to compute the geometries of the protonated starting compound, the corresponding transition-state structure, and the product. For the transition structure optimization at the DFT level, the option "mndofc" [opt = (ts, noeigentest, mndofc)] was used, applying the B3LYP/6-31G(d) basis set. All stationary points were verified by frequency analyses.

Synthesis of Compound 1. A total of 5 mg of T-2 was redissolved in 5 mL of chloroform, and 45 mL of water was added. The reaction mixture was initially heated at 80 °C to remove the chloroform. Afterward, the oil bath was heated at 175 °C, and the reaction mixture was refluxed for 6 h. The cooled solution was extracted with ethyl acetate, and the combined organic layers were dried over sodium sulfate. The reaction residue was analyzed by GC−MS and HPLC−MS/MS.

Model Baking Experiment. A stock solution of T-2 in a concentration of 1 mg/mL in acetonitrile was prepared. A total of 10 μL of this solution was added to 10 g of wheat flour type 405 and homogenized by shaking for 2 h, resulting in a concentration of 1 mg of T-2/kg of

wheat flour. Dry samples were prepared by weighing 0.6 g of T-2 spiked wheat flour in a 1.5 mL glass vial. For wet samples, 400 μL of water was added and the "dough" was thoroughly mixed. The samples were then heated in a heating block at 200 °C for 60 min, reflecting the representative temperature and time used in baking bread. The resulting crust was extracted 3 times with 1 mL of methanol and filtered through a Spartan 13/0.45 RC filter unit (Schleicher and Schuell, Dassel, Germany). The solvent was evaporated to dryness, and the residue was dissolved in 300 μL of acetonitrile/water (1:1, v/v) and analyzed by HPLC−MS/MS.

Stock Solutions. T-2, HT-2, compounds **1**, **2**, and **3**, as well as the internal standards d_3-T-2 and d_3-HT-2 were dissolved in acetonitrile. T-2, HT-2, d_3-T-2, and d_3-HT-2 were diluted with acetonitrile to a concentration of 10 μg/mL, and compounds **1**, **2**, and **3** were diluted with acetonitrile to a concentration of 1 μg/mL, respectively. The solutions were stored at −18 °C and were stable over several months.

Sample Preparation. A total of 25 g of commercially available food samples ($n = 18$) was weighed in an Erlenmeyer flask, and 625 ng of d_3-T-2 (62.5 μL of the stock solution) and 625 ng of d_3-HT-2 (62.5 μL of the stock solution) were added as an internal standard. A total of 100 mL of acetonitrile/water (84:16, v/v) was added, and the samples were homogenized with an Ultra Turrax T25B (Janke and Kunkel IKA, Staufen, Germany) for 3 min at 20 000 rpm. After filtration through a Schleicher and Schuell filter (5951/2, 320 mm), the extract was cleaned up using the method of Klötzel et al. (*20*): 4 mL of the extract was passed through a Varian Bond Elut Mycotoxin cartridge. Exactly 2 mL of the eluate was evaporated to dryness under a stream of nitrogen (42 °C), and the residue was redissolved in 500 μL of water/acetonitrile (3:2, v/v) and further analyzed by HPLC−MS/MS. For quantification, nine standard solutions containing T-2 (0.1−100 ng/mL), HT-2 (0.5−100 ng/mL), compounds **1**, **2**, and **3** (0.1−10 ng/mL), and the internal standards d_3-T-2 (25 ng/mL) and d_3-HT-2 (25 ng/mL) were prepared and analyzed by HPLC−MS/MS in the MRM mode. For the calculation of calibration curves, the peak area ratios of the analytes to the internal standard were plotted against the concentration ratios. Thereby, d_3-T-2 was used as an internal standard for T-2 and compounds **2** and **3**, while d_3-HT-2 was used for HT-2 and compound **1**.

The recovery of the method was checked by spiking a zwieback sample containing no detectable T-2, HT-2, and compounds **1**, **2**, and **3**. Spiking levels were 2 and 8 μg/kg for T-2 and HT-2, while it was 1 and 2 μg/kg for compounds **1**, **2**, and **3**. The samples were cleaned up according to the procedure described above and analyzed in duplicate by HPLC−MS/MS.

HPLC−ESI−MS/MS Analysis. For HPLC−ESI−MS/MS analysis, an Agilent 1100 series HPLC was linked to the API 4000 QTrap mass spectrometer (Applied Biosystems, Darmstadt, Germany). Data acquisition was performed with the Analyst 1.4.2 software (Applied Biosystems). Chromatographic separation was performed on a 150 × 2.00 mm i.d., 5 μm, Phenomenex Gemini 5 μm C18 100 A column (Phenomenex, Aschaffenburg, Germany) using a linear binary gradient with water and acetonitrile as eluents. The injection volume was 20 μL, and the flow rate was 200 μL/min. The HPLC was programmed as follows: isocratic step at 10% acetonitrile for 1 min followed by a linear gradient to 100% acetonitrile in 26 min. After each HPLC run, the column was washed with 100% acetonitrile for 7 min and equilibrated for 15 min at the starting conditions. For HPLC−MS/MS, the mass spectrometer was operated in the multiple reaction monitoring mode (MRM), detecting positive ions. Zero-grade air served as the nebulizer gas (30 psi) and was heated at 300 °C, as turbo gas for solvent drying (50 psi). The following transition reactions were monitored for a duration of 150 ms each. Declustering potential (DP), collision energy (CE), and collision cell exit potential (CXP) are given in parentheses.

Baking experiment: T-2 and compounds **2** and **3**, 484.3−305.1 (DP, 61 V; CE, 21 V; CXP, 8 V); compound **1**, 502.2−425.1 (DP, 61 V; CE, 21 V; CXP, 12 V).

Food samples: T-2, 484.3−305.1 (DP, 61 V; CE, 21 V; CXP, 8 V); HT-2, 442.3−263.1 (DP, 46 V; CE, 19 V; CXP, 6 V); compound **1**, 502.2−425.1 (DP, 61 V; CE, 21 V; CXP, 12 V); compound **2**, 484.3−305.1 (DP, 61 V; CE, 21 V; CXP, 8 V); compound **3**, 484.2−365.1 (DP, 56 V; CE, 13 V; CXP, 16 V); d_3-T-2, 487.3−308.1 (DP, 61 V; CE, 21 V; CXP, 8 V); d_3-HT-2, 445.3−263.1 (DP, 46 V; CE, 19 V; CXP, 6 V).

Cell Culture. Immortalized human kidney epithelial cells (IHKE cells, passage 154−157) were kindly provided by M. Gekle (Würzburg, Germany) (IHKE cells are originally from S. Mollerup, National Institute of Occupational Health, Norway). They were cultured as described by Tveito et al. (*21*) in Dulbecco's modified Eagle's medium (DMEM)/Ham's-F12 medium (100 μL/cm^2) enriched with 13 mmol/L $NaHCO_3$, 15 mmol/L *N*-2-hydroxylethylpiperazine-*N*′-2-ethanesulfonic acid (HEPES), 36 μg/L hydrocortisone, 5 mg/L human apotransferrin, 5 mg/L bovine insulin, 10 μg/L mouse epidermal growth factor, 5 μg/L Na selenite, 10% fetal calf serum, and in addition, 1% penicillin/streptomycin under standard cell culture conditions (37 °C, 5% CO_2).

Cytotoxicity Assay. Cytotoxicity was evaluated colorimetrically with the Cell Counting Kit-8 (CCK-8) from Dojindo Laboratories (Tokyo, Japan) similar to the instructions of the manufacturer. Briefly, cells were grown on a 96-well microplate. A total of 100 μL of a cell suspension, containing 3×10^3 cells, was added to each well. After 48 h of growth, culture medium was replaced by serum-free medium for 24 h. Test compounds were dissolved in acetonitrile and added to serum-free medium (the final acetonitrile concentration was <1%). After 24 h of incubation, the WST-8 [2-(2-methoxy-4-nitrophenyl)-3-(4-nitrophenyl)-5-(2,4-disulfophenyl)-2*H*-tetrazolium, monosodium salt] solution was added and the cells were incubated for 1 h. WST-8 produces a water-soluble formazan dye upon reduction in the presence of an electron carrier. The absorbance of each well was measured with a FLUOstar Optima microplate reader (BMG Labtechnologies, Jena, Germany) at 450 nm. The amount of the formazan generated by the activity of dehydrogenases in cells is directly proportional to the number of viable cells per well. The absorbance of the treated wells was compared to the solvent-treated control. The medium effective concentrations (EC_{50} values) were calculated using SigmaPlot 8.0 according to DeLean et al. (*22*).

RESULTS AND DISCUSSION

Model Experiments. In an attempt to obtain more information about the fate of T-2 under typical food-processing conditions, heating experiments with model substances simulating typical food constituents were performed. To study the formation of degradation and reaction products as well as the binding of T-2 to food constituents, it was heated with the following model substances: α-D-glucose as a sugar model, methyl-α-D-glucopyranoside as a starch model, and the amino acid derivates *N*-α-acetyl-L-lysine methyl ester and *N*-acetyl-L-cysteine methyl ester as protein models. T-2 was heated with the model substances at various temperatures (150−200 °C) for different time periods (5−60 min), and the reaction residues were analyzed by GC−MS as well as HPLC−ELSD. Degradation of T-2 was observed under all conditions, generally accelerating with rising temperatures. The strongest degradation of T-2 was found in the protein models. After heating for 60 min at 175 °C, only 30% T-2 was left with the *N*-acetyl-L-cysteine methyl ester and 40% with the *N*-α-acetyl-L-lysine methyl ester; in comparison, it was 70% when pure T-2 was heated (**Figure 2A**). Although degradation of T-2 was very fast in the presence of the protein models, there were no degradation products detectable with HPLC−ELSD. Because the losses in the heating experiments with the amino acid derivatives cannot be ascribed to the formation of degradation products, they are most likely caused by polymerization or pyrolysis reactions. In comparison, the degradation of T-2 by heating with α-D-glucose and methyl-α-D-glucopyranoside was not so strong. After heating for 60 min at 175 °C, 50% T-2 remained with methyl-α-D-glucopyranoside and 60% remained with α-D-glucose (**Figure 2B**), but in the heating experiment with α-D-glucose,

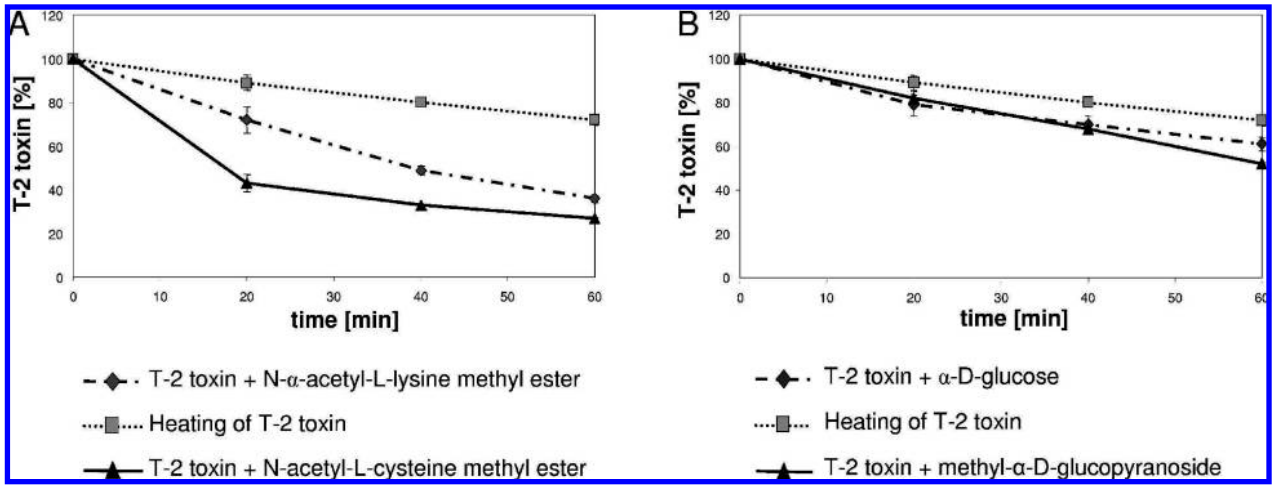

Figure 2. Degradation of T-2 toxin at 175 °C with (A) *N*-α-acetyl-L-lysine methyl ester and *N*-α-acetyl-cysteine methyl ester and (B) α-D-glucose and α-D-methylglucopyranoside.

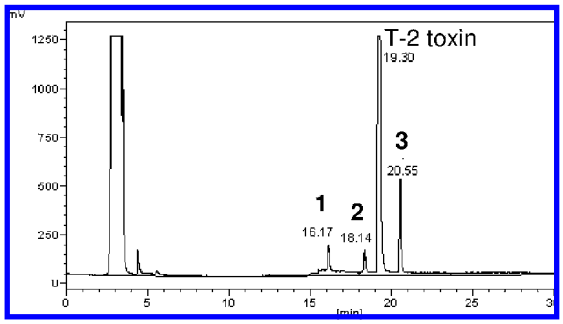

Figure 3. HPLC−ELSD chromatogram of T-2 toxin heated with α-D-glucose for 1 h at 175 °C.

only three degradation products of T-2 were detectable with HPLC−ELSD in appreciable amounts (**Figure 3**). These degradation products were also formed by heating T-2 alone but in much lesser amounts.

Structural Identification of the Degradation Products. For the preparative isolation of the new compounds, T-2 was heated with α-D-glucose at 200 °C for 6 h to increase yields of the degradation products. For structure elucidation, they were isolated by preparative HPLC and analyzed by ESI−TOF−MS, ESI−MS/MS, GC−MS, and several NMR experiments, such as ^{1}H, ^{13}C, and 1D NOE, DEPT-135, and different 2D NMR experiments, such as H,H COSY, H,C HMQC, and H,C HMBC. The structures of the T-2 degradation products are shown in **Figure 4**. ESI−MS/MS analysis showed that the two acetyl groups as well as the isovaleroyl group remained in all of the T-2 degradation products.

In comparison to T-2, compound **1** (yield, 9.8 mg collected from several batches), for which the systematic name is 4,15-diacetoxy-10,12-cyclohexa-(10*H*)-3,9,12-trihydroxy-8-[3-methylbutyryloxy]-trichothecene, contains two additional hydroxy groups. This was confirmed by GC−MS analysis of the silylated molecule. As the exact mass of compound **1** is 18 amu greater than that of T-2; a first hint for water addition in the molecule was given. In the ^{13}C NMR spectrum of compound **1**, the characteristic shifts for the double bond are missing; instead, two new shifts for C-9 and C-10 at 72.5 and 42.7 ppm originated, concluding that the unsaturated character is lacking. In accordance with the exact mass of compound **1** and the chemical shift of C-9, it was suggested that an additional hydroxy group is present at C-9. Besides, H-10 is upshifted to 2.30 ppm, which showed couplings to H-11 (3.74 ppm) and two other protons at 1.59 and 1.88 ppm allocated as H-13A and H-13B by COSY and HMBC experiments. Moreover, C-13 is upshifted to 27.7 ppm, while C-12 is downshifted to 76.7 ppm, suggesting that the epoxy group is missing as well. Instead, a new bond between C-13 and C-10 and a hydroxy group at the quarternary carbon atom C-12 are detectable. The GC−MS spectrum of compound **1** showed two peaks with the same molecular ion as well as the same fragmentation pattern, showing that compound **1** is a mixture of two diastereomers, differing at the stereocenter at C-9, which was confirmed by NMR analysis. The diastereomers are generated in the ratio of 86:14, and because both diastereomers showed nearly identical shifts in the ^{1}H as well as in the ^{13}C spectrum, only the data of the principal diastereomer are shown.

The structure of compound **2** (yield, 4.7 mg collected from several batches), named 4,15-diacetoxy-10,12-cyclohexa-(10*H*)-3,12-dihydroxy-8-[3-methylbutyryloxy]-9-methylidene-trichothecene coincides with the structure of compound **1**, varying only at position C-9. The ^{13}C NMR spectrum showed shifts for C-9 and C-16 at 146.0 and 106.1 ppm, respectively. Therefore, it was concluded that a double bond between C-9 and C-16 occurs, which is consistent with the exact mass and the number of hydroxy groups of compound **2**. Compound **3** (yield, 7.9 mg collected from several batches), with the systematic name 4-acetoxy-9,10-cyclopropyl-3,15-dihydroxy-8-[3-methylbutyryloxy]-12-oxotrichothecene, has in contrast to T-2 a keto group at C-12 because the shift of this quarternary carbon atom is

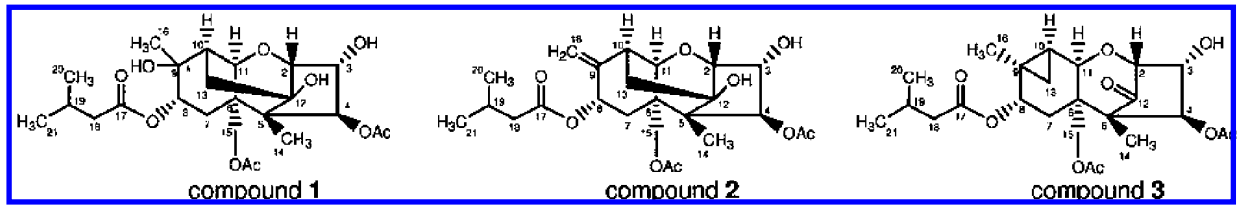

Figure 4. Structures of the T-2 toxin degradation products.

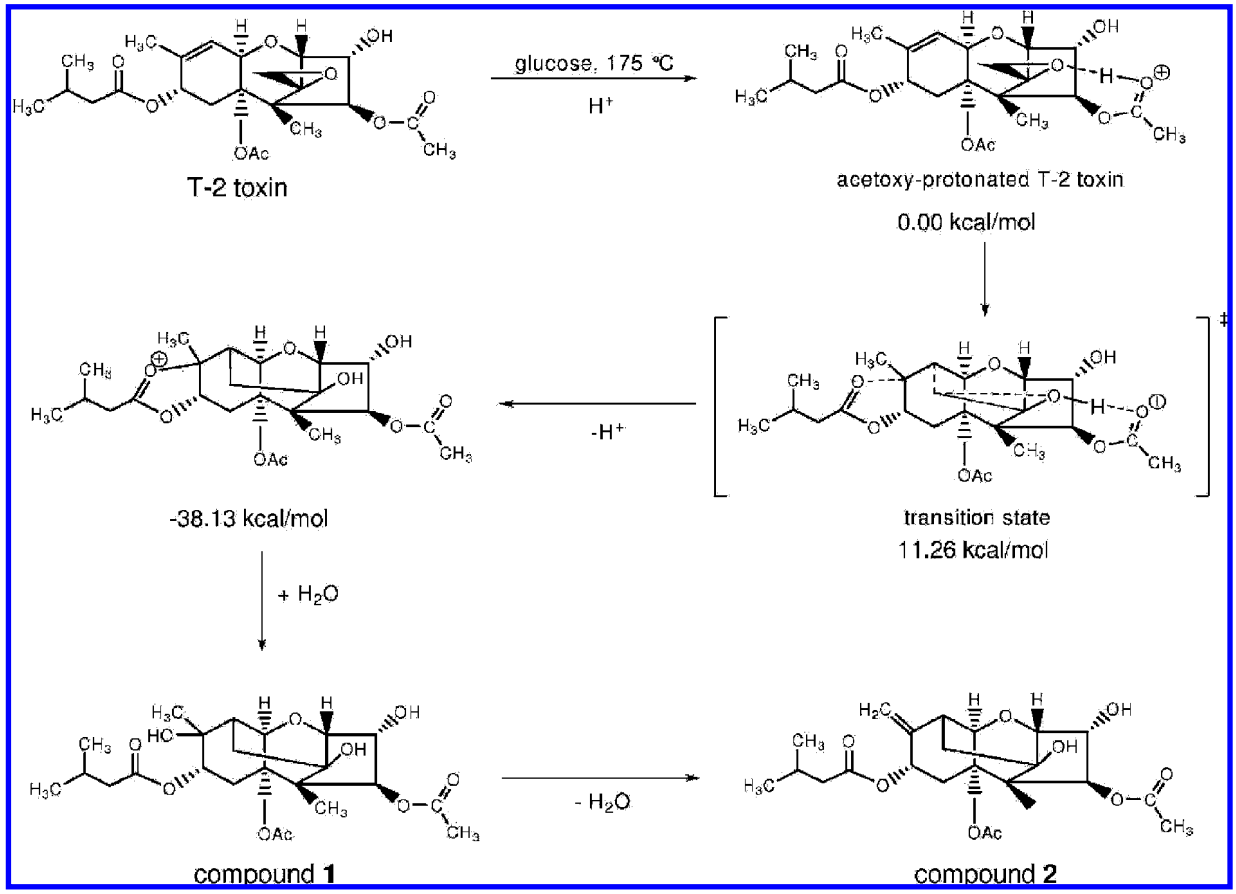

Figure 5. Calculated reaction pathway for the formation of the T-2 toxin degradation products.

downshifted to 209.6 ppm. In contrast, the shift of C-13 was upshifted to 14.1 ppm. Together with the shifts of H-13A at 0.59 ppm and H-13B at 0.84 ppm, this is only explicable as a result of a highly strained ring system. In conclusion, a new cyclopropane ring system is present, which is located between C-9, C-10, and C-13, discovered by 2D NMR experiments.

Possible Reaction Pathway. To clarify the reaction pathway (**Figure 5**) for the formation of the T-2 degradation products, quantum chemical calculations were performed, which are based on the assumption that T-2 is available in an acetoxy-protonated form. This might be rationalized by the fact that T-2 is heated in the presence of aqueous glucose. The protonated acetoxy group is able to form a hydrogen bond to the oxygen atom of the epoxy moiety. On the basis of this reactant (E_{rel} = 0.0 kcal/mol), a reaction pathway was calculated, where the essential α-carbon atom of the C═C double bond is attacked by the electrophilic carbon atom of the protonated oxirane. From this reaction pathway, a transition state was localized, which is only 11.3 kcal/mol higher in energy than the reactant. The developing positive charge in this transition state is significantly stabilized by the interaction with the oxygen atom of the isovaleroyl group. Thus, this very rational transition state involves many of the functional groups of the molecule, and its favorable energy is a result of a least six interacting bonds, well-distributed over the entire surface of the molecule. The continuation of this pathway results in a cationic species incorporating a dioxolanium ring. This reaction is predicted to be very exothermic (−38.1 kcal/mol), particularly because of the cancelation of the oxirane ring strain. In the course of the reaction, this positively charged intermediate is hydrolyzed to give compound **1**. Water elimination from compound **1** affords compound **2** (ca. 38.4 kcal/mol lower than T-2 at PM6). Compound **3** (ca. 20.6 kcal/mol lower in energy than T-2 at PM6) might either be generated from

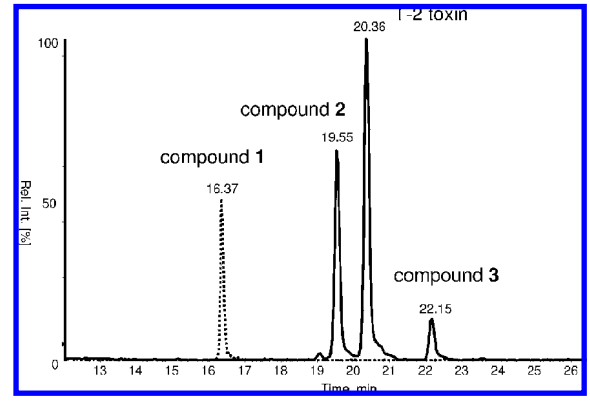

Figure 6. HPLC−ESI−MS/MS analysis of a flour sample spiked with 1 mg/kg T-2 toxin heated for 1 h at 200 °C.

compound **2** or, more likely, from the intermediate, which results from the transition state of the proton-catalyzed rearrangement reaction.

Because an analogous product to compound **1** was formed by heating of triacetoxyscirpene in water (*23*), we heated T-2 for 6 h under reflux in an oil bath at 175 °C. HPLC−MS/MS as well as GC−MS analysis of the reaction mixture showed that, besides HT-2, compound **1** was produced by the reaction of T-2 with water, while compounds **2** and **3** were not generated. As in our model experiments, compound **1** was obtained as a mixture of two diastereomers.

Degradation of HT-2 Toxin. Because the structures of T-2 and HT-2 are closely related, it is reasonable that comparable degradation products will be generated by heating of HT-2 with α-D-glucose as well. To confirm this assumption, we heated HT-2 with α-D-glucose for 1 h at 200 °C and screened the

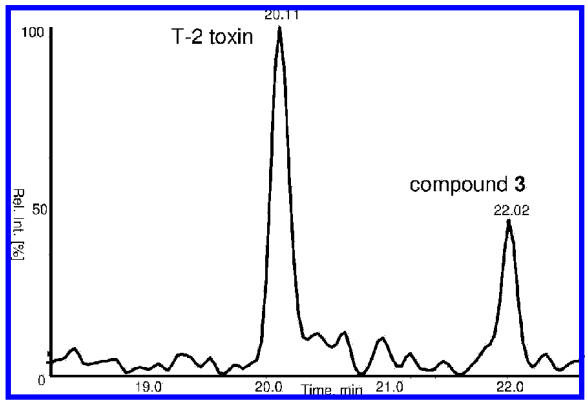

Figure 7. HPLC−ESI−MS/MS analysis of a wholemeal pastries sample.

reaction residue with HPLC−MS in the positive scan mode. Besides HT-2, there was one additional peak with a signal 18 amu higher compared to HT-2. This finding is a first hint that a degradation product comparable to compound **1** is generated by heating of HT-2 with α-D-glucose. However, the structure could not be confirmed by NMR analysis during our studies, because the availability of HT-2 was limited.

Presence of the Degradation Products in Food Samples. To study the formation of T-2 degradation products in real samples, we spiked flour with 1 mg/kg T-2 and heated the samples both with and without added water. The samples were extracted with methanol, filtered, and further analyzed by HPLC−MS/MS. **Figure 6** shows the associated chromatogram of the flour sample heated without water for 1 h at 200 °C, mimicking the conditions during the process of baking bread. The chromatogram of the model baking experiment showed the formation of the T-2 degradation products in the heat-treated flour, whereby no significant difference between heating with and without water was detected. After heating with water, 21% T-2 remained, while it was 14% without water. The concentrations of the degradation products are approximately 10−20% of the initial concentration of T-2. Because of higher ionization efficiency, the signal intensities of compounds **1** and **2** are higher than that of compound **3**.

After the detection of the degradation products in model baking experiments, we examined the occurrence of the degradation products in commercially available food samples. Therefore, a total of 18 thermally processed samples, such as different pastries or tortilla chips from the German retail market, were analyzed in duplicate. Main ingredients in all samples were wheat, maize, or oats. The samples were homogenized, spiked with d_3-T-2 and d_3-HT-2 as internal standards, and extracted with acetonitrile/water (84:16). The extract was filtered and purified using a Bond Elut Mycotoxin cartridge. After a further concentration step, the sample was analyzed by HPLC−MS/MS.

Table 1. Concentration of HT-2, T-2, and Compound **3** in Thermally Treated Food Samples

		concentration (μg/kg)		
sample	main ingredients	HT-2	T-2	compound **3**
wholemeal pastries 1	wheat	<0.5	0.3	<0.1
wholemeal pastries 2	wheat, oats, rice	0.9	0.9	nd[a]
wholemeal pastries 3	wheat, barley	nd[a]	<0.1	<0.1
wholemeal pastries 4	wheat	<0.5	<0.1	nd[a]
wholemeal pastries 5	wheat, rye	1.0	0.1	<0.1
wholemeal pastries 6	wheat	<0.5	0.1	nd[a]
crispbread	wheat	<0.5	<0.1	nd[a]
zwieback	wheat	nd[a]	nd[a]	nd[a]
cornflakes	maize, barley	nd[a]	<0.1	nd[a]
tortilla chips 1	maize	0.6	0.6	nd[a]
tortilla chips 2	maize	0.8	0.1	nd[a]
tortilla shells	maize	<0.5	<0.1	nd[a]
oat pastries 1	oats, spelt	1.8	0.9	nd[a]
oat pastries 2	oats, wheat	3.5	1.7	nd[a]
oat pastries 3	oats, wheat	3.3	1.9	nd[a]
oat cookies 1	oats	4.4	1.2	nd[a]
oat cookies 2	oats, wheat	<0.5	1.1	nd[a]
oat-rice cookies	oats, wheat, rice	<0.5	0.4	nd[a]
positive samples (>LOQ)		8	12	
mean (positive samples)		2.0	0.8	
median		1.4	0.8	

[a] nd = not detectable.

The recovery rates were determined in zwieback matrix spiked at 2 and 8 μg/kg for T-2 and HT-2, as well as 1 and 2 μg/kg for compounds **1**, **2**, and **3**. For each concentration level, two samples were worked up independently. The recovery rates for T-2 were 100.8 ± 6.0 and 102.5 ± 5.5%, and the recovery rates for HT-2 were 92.0 ± 1.4 and 104.2 ± 6.9% for the spiking levels 2 and 8 μg/kg, respectively. The recovery rates for compound **1** were 109.8 ± 8.8 and 103.5 ± 14.8%; the recovery rates for compound **2** were 108.0 ± 27.9 and 104.5 ± 4.2%; and recovery rates for compound **3** were 81.2 ± 3.8 and 70.5 ± 2.8% for the spiking levels 1 and 2 μg/kg, respectively.

In **Table 1**, the results of the analyzed food samples are shown. T-2 was detected in 17 of the 18 analyzed samples, albeit in 5 samples in concentrations <0.1 μg/kg (limit of quantification, LOQ) and in the other samples in concentrations <2 μg/kg. The highest amount of T-2, which was detected in an oat pastries sample, was 1.9 μg/kg. On the basis of the low amounts of T-2 in the analyzed samples, concentrations of T-2 degradation products are easily under the limit of detection. Nevertheless, compound **3** was detected in three of the analyzed samples, but in concentrations <0.1 μg/kg, which was the limit of quantification. A representative chromatogram of wholemeal

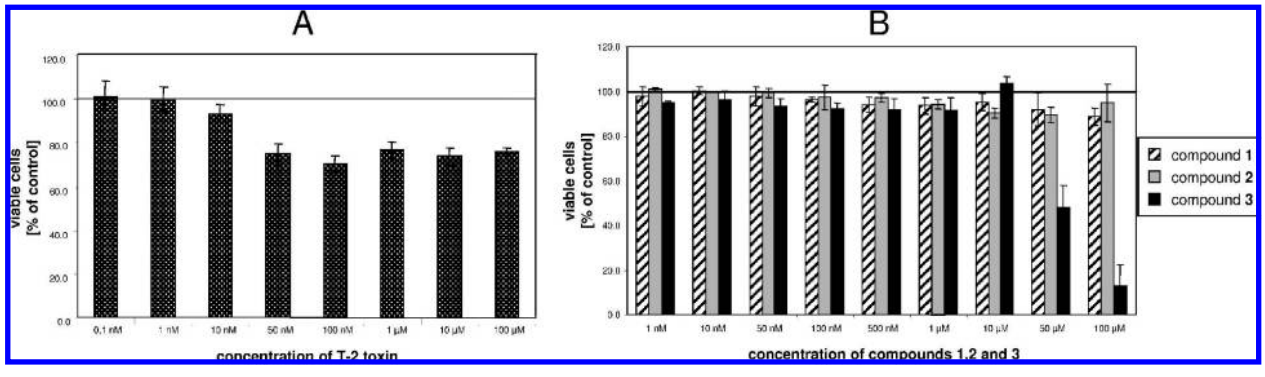

Figure 8. Cytotoxicity of (A) T-2 toxin and (B) the T-2 toxin degradation products on IHKE cells.

pastries is shown in **Figure 7**. Compounds **1** and **2** were not detectable in the analyzed samples, but the occurrence of compound **3** in food samples showed the relevance of T-2 degradation products. In addition, the HT-2 concentrations in the samples were analyzed as well. HT-2 was detected in 15 of the 18 analyzed samples, thereof in seven samples in concentrations 0.5 μg/kg (LOQ). The highest amount of HT-2 was 4.4 μg/kg, detected in oat cookies.

Cytotoxicity of the Degradation Products. Because the three degradation products were generated during the baking experiment and compound **3** was additionally detected in food samples of the German retail market, we have determined their cytotoxicity in cell-culture experiments using IHKE cells. As shown in **Figure 8**, T-2 revealed a median effective concentration (EC_{50}) at approximately 19 $\pm$ 1.6 nM, which is in a similar range compared to literature data (*24*). In contrast, compounds **1** and **2** did not exhibit any significant effect up to 100 μmol. The only compound showing a cytotoxic effect on IHKE cells was compound **3**. The calculated EC_{50} value for this compound is 47 $\pm$ 7.0 μM, which is more than 1000-fold higher than that of T-2 toxin (**Figure 8**). These results are consistent with the fact that the epoxy group plays a major role in the cytotoxicity of trichothecenes (*25*, *26*). Injection (i.p.) of 60 mg of de-epoxy T-2/kg of bw did not show any significant effect in rats, whereas seven of nine rats died after injection of 12 mg of T-2/kg of bw (*27*). In the rat skin irritation bioassay, de-epoxy T-2 was less toxic than T-2 toxin by a factor of more than 400 (*28*). Consistent results were obtained for the type-B trichothecenes deoxynivalenol and nivalenol and their respective de-epoxides. In cell-culture experiments using the 5-bromo-2′-deoxyuridine incorporation assay accessing DNA synthesis, it was demonstrated that the de-epoxides of deoxynivalenol and nivalenol were 24 and 52 times less toxic compared to deoxynivalenol and nivalenol with an intact epoxide ring (*24*). Furthermore, the de-epoxides are much less acutely toxic than the corresponding trichothecenes, which was shown in the brine shrimp bioassay (*26*). Furthermore, cell-culture investigations of our group showed that the degradation of deoxynivalenol and nivalenol is associated with less cytotoxic degradation products (*11*, *12*).

SUMMARY

Model experiments were performed to study the stability of T-2 under food-processing conditions. Three degradation products were identified in a model system, and their structures as well as the reaction pathway were elucidated. In cell-culture studies, the three T-2 degradation products were less cytotoxic compared to T-2. At least one degradation product (compound **3**) was identified in three different samples from the German retail market. However, it has to be mentioned that the available samples contained only low concentrations of T-2 toxin (<2 μg/kg), and for this reason, the relevance of the T-2 degradation products in food samples cannot be finally answered from our data. The analysis of higher T-2-contaminated samples has to be performed in the future.

ABBREVIATIONS USED

ATA, alimentary toxic aleukia; CCK-8, Cell Counting Kit-8; DEPT-135, distortionless enhancement by polarization transfer using a 135° decoupler pulse; HMBC, heteronuclear multiple-bond correlation; HMQC, heteronuclear multiple-quantum correlation; HT-2, HT-2 toxin; IHKE cells, immortalized human kidney epithelial cells; LOQ, limit of quantification; T-2, T-2 toxin; NOE, nuclear Overhauser effect.

ACKNOWLEDGMENT

We thank H. Luftmann for the exact mass measurements and K. Bergander for setting up the 1D NOE NMR experiments.

LITERATURE CITED

(1) European Commission, Scientific Committee on Food, Opinion of the Scientific Committee on Food on *Fusarium* Toxins, Part 6: Group Evaluation of T-2 Toxin, HT-2 Toxin, Nivalenol and Deoxynivalenol, 2002, http://europa.eu.int/comm/food/fs/sc/scf/out123_en.pdf (accessed on Dec 16, 2008).

(2) Middlebrook, J. L.; Leatherman, D. L. Binding of T-2 toxin to eukaryotic cell ribosomes. *Biochem. Pharmacol*. **1989**, *38*, 3103–3110.

(3) Thompson, W. L.; Wannemacher, R. W., Jr. Structure−function relationships of 12,13-epoxytrichothecene mycotoxins in cell culture: Comparison to whole animal lethality. *Toxicon* **1986**, *24*, 985–994.

(4) European Commission, Scientific Committee on Food, Opinion of the Scientific Committee on Food on *Fusarium* Toxins, Part 5: T-2 Toxin and HT-2 Toxin, 2001, http://europa.eu.int/comm/food/fs/sc/scf/out88_en.pdf (accessed on Dec 16, 2008).

(5) Joint FAO/WHO Expert Committee on Food Additives (JECFA). Safety evaluation of certain food additives. WHO Food Additives Series 47, 2001, http://www.inchem.org/documents/jecfa/jecmono/v47je01.htm (accessed on Dec 16, 2008).

(6) Bennett, J. W.; Klich, M. Mycotoxins. *Clin. Microbiol. Rev*. **2003**, *16*, 497–516.

(7) Kamimura, H. Removal of mycotoxins during food processing. In *Mycotoxins and Phycotoxins*, *88*; Natori, S., Hashimoto, K., Ueno, Y., Eds.; Elsevier Science Publisher: Amsterdam, The Netherlands, 1989.

(8) Kamimura, H. N., M.; Saito, K.; Yasuda, K.; Ibe, A.; Nagayama, T.; Ushiyama, H.; Naoi, Y. Studies on mycotoxins in foods. XII. The decomposition of trichothecene; mycotoxins during food processing. *Shokuhin Eiseigaku Zasshi* **1979**, 352–357.

(9) Lauren, D. R.; Smith, W. A. Stability of the *Fusarium* mycotoxins nivalenol, deoxynivalenol, and zearalenone in ground maize under typical cooking environments. *Food Addit. Contam*. **2001**, *18*, 1011–1016.

(10) Boyacioglu, D.; Hettiarachchy, N. S.; D'Appolonia, B. L. Additives affect deoxynivalenol (vomitoxin) flour during breadbaking. *J. Food Sci*. **1993**, *58*, 416–418.

(11) Bretz, M.; Beyer, M.; Cramer, B.; Knecht, A.; Humpf, H. U. Thermal degradation of the *Fusarium* mycotoxin deoxynivalenol. *J. Agric. Food Chem*. **2006**, *54*, 6445–6451.

(12) Bretz, M.; Knecht, A.; Goeckler, S.; Humpf, H. U. Structural elucidation and analysis of thermal degradation products of the *Fusarium* mycotoxin nivalenol. *Mol. Nutr. Food Res*. **2005**, *49*, 309–316.

(13) Abbas, H. K.; Mirocha, C. J.; Rosiles, R.; Carvajal, M. Decomposition of zearalenone and deoxynivalenol in the process of making tortillas from corn. *Cereal Chem*. **1988**, *65*, 15–19.

(14) Koenigs, M.; Mulac, D.; Humpf, H. U. Metabolism of T-2 toxin and cytotoxic effects of its metabolites on human cells in primary culture. *Toxicology* **2009**, accepted for publication.

(15) Gottschalk, C.; Barthel, J.; Engelhardt, G.; Bauer, J.; Meyer, K. Occurrence of type A trichothecenes in conventionally and organically produced oats and oat products. *Mol. Nutr. Food Res*. **2007**, *51*, 1547–1553.

(16) Seefelder, W.; Knecht, A.; Humpf, H. U. Bound fumonisin B1: Analysis of fumonisin-B1 glyco and amino acid conjugates by liquid chromatography−electrospray ionization−tandem mass spectrometry. *J. Agric. Food Chem*. **2003**, *51*, 5567–5573.

(17) Stewart, J. J. P. Optimization of parameters for semiempirical methods V: Modification of NDDO approximations and application of 70 elements. *J. Mol. Model*. **2007**, *13*, 1173–1213.

(18) Stewart, J. J. P. MOPAC 2007, Stewart Computational Chemistry, Colorado Springs, CO, 2007 (http://OpenMOPAC.net).

(19) Frisch, M. J. Gaussian 03, Revision D.01, Gaussian, Inc., Wallingford CT, 2004.

(20) Kloetzel, M.; Lauber, U.; Humpf, H. U. A new solid phase extraction clean-up method for the determination of 12 type A and B trichothecenes in cereals and cereal-based food by LC−MS/MS. *Mol. Nutr. Food Res.* **2006**, *50*, 261–269.
(21) Tveito, G.; Hansteen, I. L.; Dalen, H.; Haugen, A. Immortalization of normal human kidney epithelial cells by nickel(II). *Cancer Res.* **1989**, *49*, 1829–1835.
(22) DeLean, A.; Munson, P. J.; Rodbard, D. Simultaneous analysis of families of sigmoidal curves: Application to bioassay, radioligand assay, and physiological dose−response curves. *Am. J. Physiol.* **1978**, *235*, E97–102.
(23) Sigg, H. P.; Mauli, R.; Flury, E.; Hauser, D. Die konstitution von diacetoxyscirpenol. *Helv. Chim. Acta* **1965**, *48*, 962–988.
(24) Gutleb, A. C.; Morrison, E.; Murk, A. J. Cytotoxicity assays for mycotoxins produced by *Fusarium* strains: A review. *Environ. Toxicol. Pharmacol.* **2002**, *11*, 309–320.
(25) Rotter, B. A.; Prelusky, D. B.; Pestka, J. J. Toxicology of deoxynivalenol (vomitoxin). *J. Toxicol. Environ. Health* **1996**, *48*, 1–34.
(26) Sundstol Eriksen, G.; Pettersson, H.; Lundh, T. Comparative cytotoxicity of deoxynivalenol, nivalenol, their acetylated derivatives and de-epoxy metabolites. *Food Chem. Toxicol.* **2004**, *42*, 619–624.
(27) Swanson, S. P.; Helaszek, C.; Buck, W. B.; Rood, H. D., Jr.; Haschek, W. M. The role of intestinal microflora in the metabolism of trichothecene mycotoxins. *Food Chem. Toxicol.* **1988**, *26*, 823–829.
(28) Swanson, S. P.; Rood, H. D., Jr.; Behrens, J. C.; Sanders, P. E. Preparation and characterization of the deepoxy trichothecenes: Deepoxy HT-2, deepoxy T-2 triol, deepoxy T-2 tetraol, deepoxy 15-monoacetoxyscirpenol, and deepoxy scirpentriol. *Appl. Environ. Microbiol.* **1987**, *53*, 2821–2826.

Received for review November 10, 2008. Revised manuscript received December 22, 2008. Accepted December 23, 2008. We thank the Ministry of the Environment and Conservation, Agriculture and Consumer Protection of the State of North Rhine-Westphalia for financial support.

JF803516S